# PREDICTION OF RESISTIVE SOOT SENSOR BEHAVIOR IN DIESEL EXHAUST VIA 3D SIMULATION OF SOOT DEPOSITION

**[1] Pavlos Fragkiadoulakis[*], [1] Dimitris Mertzis, [1]Savas Geivanidis, [1]Zissis Samaras**
[1] Laboratory of Applied Thermodynamics, Dept. of Mechanical Engineering, Faculty of Engineering, Aristotle University of Thessaloniki (http://lat.eng.auth.gr)
E-mail: pavfrang@auth.gr

KEYWORDS –

*Soot sensor, OBD, diesel particulate filter, CFD, physical model*

ABSTRACT –

Soot sensors are the latest tool developed in order to track diesel particulate filter (DPF) failure, which may result in excess PM emissions, the acceptable limits of which become stricter for new vehicles according to regulations. Resistive electrode/accumulating sensors are a cost-effective approach to accurately estimate soot concentration in diesel engine exhaust. Understanding the soot deposition mechanisms of a resistive sensor is a necessary step to predict and interpret the soot sensor behavior.
In this direction, a 1D transient model has been developed in order to simulate the deposition mechanisms efficiently. The exhaust gas flow field around the soot sensor is an input for the model and it is calculated through a 3D CFD model. Through this coupling, accurate data on mass flow, velocity and turbulence characteristics at the soot sensor are calculated and enhance the model's predictive capability.
According to the simulations, Brownian diffusion, thermophoresis and electrophoresis seem to primarily affect the soot accumulating rate on the sensor element. In addition, the model results agree with measurements on actual diesel engine exhaust system. The developed model correctly predicts the behavior of the sensor for a set of exhaust flow conditions and sensor properties, such as its geometry. This way, experiment costs related to the calibration process of the sensor signal are minimized and moreover the application of similar sensors on modern diesel vehicles is accelerated.
The 3D model geometry and finite element analysis have been created with the pre-processor ANSA. The CFD analysis has been carried out with ANSYS Fluent and the results are analyzed via the μETA post-processor.

TECHNICAL PAPER –

## 1. INTRODUCTION

With soot sensors, the challenge of diagnosing a DPF malfunction, is the ultimate challenge. The main advantage of a soot sensor in comparison to other sensors is its low unit cost. For the purpose of modeling a prototype soot sensor signal, a CFD model has been developed in order to investigate the flow field inside the sensor tip. The CFD results are used in support of a physical deposition model of the soot particles on the sensor electrode/plate surface. The main deposition mechanisms that have been examined are electrophoresis, thermophoresis and Brownian diffusion
The main advantage of a physical versus an empirical model of the soot sensor response, is the underlying understanding of these deposition mechanisms that rule the physics inside the sensor tip. Moreover, further understanding of the flow inside the tip is important in order to select the proper housing tip that maximizes the measuring capabilities of the sensor.

## 2. SOOT SENSOR OPERATION

Soot sensors are used in order to instantaneously estimate the amount of accumulated soot, so that the engine management in an automobile (OBD) can receive information about the current status of a DPF with the aid of control technology adaptations.

Sensor operation principles

A resistive soot sensor typically includes a plate-like layer, used as a substrate (3), which contains a highly insulating material from a ceramic, such as aluminium oxide ($Al_2O_3$). The comb-like electrode structure which resides upon the ceramic layer (Figure 1), is generally formed by thin conductor tracks lying next to another (4). Dendrites are formed by deposited soot particles between two electrodes (Figure 2). As the soot particles accumulate on the interelectrode surface, the conductivity of the electrodes increases until a specific point, where saturation takes place. Periodically, a heating element at the opposite side of the ceramic assists in cleaning the element through oxidation of the accumulated soot.

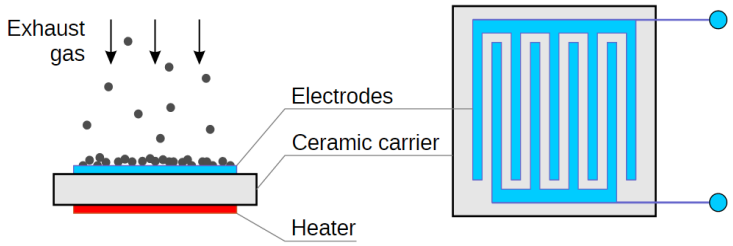


Figure 1 **–** Schematic of soot sensing principle (5)

There are three phases during the sensor operation, which are typical for every resistive accumulating sensor:

- Phase 1 - Dead Band: during this phase the sensor is loading, however the deposited particles are not adequate in order for the sensor to generate a reliable signal.
- Phase 2 - Sensing Period: after an internal threshold of the sensor has been passed, the sensor starts showing a signal which continues to increase as the sensor continues to accumulate soot. The sum of the duration of the Dead Band and of the Sensing Period defines the sensor “response time”, which is the physical quantity to be further utilized from the OBD system.
- Phase 3 - Regeneration Phase: The sensor conductivity/current reaches a threshold and the sensor is not capable to measure any more. In this phase, the soot particles are removed from the electrodes. The heater increases temperature to initiate soot oxidation at a temperature which is greater than 600°C. The soot is removed via burning and after this phase, the sensor is ready to accumulate particles again (Phase 1).

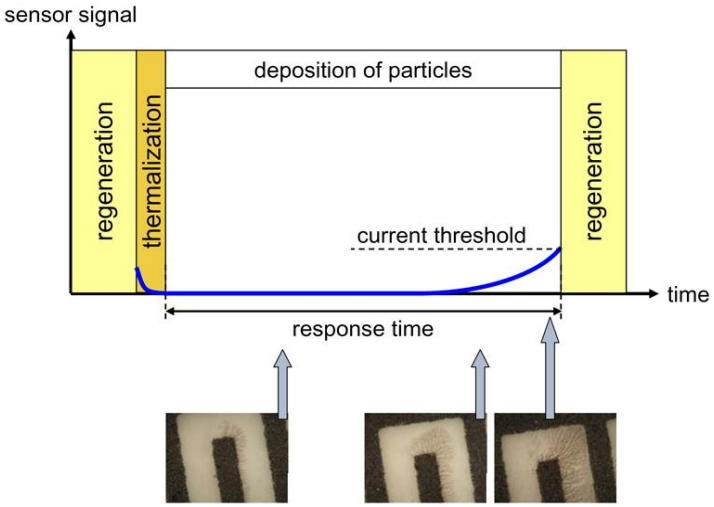


Figure 2 **–** The phases of the sensor signal as the soot begins to accumulate on the electrodes (6). As dendrites become larger, the electrode conductance (and thus the current) increases with a rate that depends on the exhaust gas parameters.

## 2. DEPOSITION MODELS

The sensor signal increases as the soot particles accumulate on the electrodes surface. The response time of the sensor, which has been defined as the time between two consecutive regenerations, depends on the deposition rate of the soot particles. The main quantity that quantifies the deposition phenomenon is called deposition velocity which is defined as: the ratio of the deposition particle flux over the initial particle concentration (7):

$$V_{dep} = \frac{J}{n_0}$$

*Where:* *J: particle deposition flux [(number of particles) / (m²s)]*
*$n_0$: undisturbed concentration [(number of particles)/m³]*

The deposition mechanisms that mainly affect the sensor response time are thermophoresis, electrophoresis and Brownian diffusion as explained below. Other mechanisms that need validation and CFD data regarding their inputs are Inertial Impaction and Turbulent Impaction.

Turbulent impaction

When a turbulent gas carrying particles with aerodynamic diameter larger than about 1 μm flows parallel to a surface, particles deposit because of the fluctuating velocity components normal to the surface (8). The effect of turbulent impaction is not expected to be significant because of the small particle diameter which is mostly below 100 nm for soot particles. Besides, the turbulent intensity is needed in order to quantify its effect. To calculate the turbulent impaction deposition velocity, the friction velocity is needed which is approximated as the rms value of velocity (8):

$$u^* \approx u_{rms} = I \cdot V$$

*Where:* *u*: friction velocity [m/s]*
*I: turbulent intensity [-]*
*V: exhaust gas velocity [m/s]*

Besides, the particle relaxation time is given by:

$$\tau_p = \frac{\rho_p d_p^2 C_c}{18 \mu_g}$$

*Where:* *$\tau_p$: particle relaxation time [s]*
*$\rho_p$: particle density [kg/m³]*
*$d_p$: particle equivalent diameter [m]*
*$C_c$: Cunningham slip correction factor [-]*
*$\mu_g$: dynamic viscosity of the gas [Ns/m²]*

Finally, the turbulent impaction deposition velocity is calculated below:

$$V_t = u^* \min\left[ 6 \cdot 10^{-4} \cdot \left( \frac{\tau_p}{\frac{v_g}{(u^*)^2}} \right), 0.1 \right]$$

*Where:* *u*: friction velocity [m/s]*
*$\tau_p$: particle relaxation time [s]*
*$v_g$: kinematic viscosity of the gas [m²/s]*

Inertial Impaction

Inertial impaction deposition is based on the phenomenon that particles whose inertia exceeds a certain value, are unable to follow the streamlines of the carrier gas and collide (impact) on the plate (7). The plate is called in general the “impaction plate” and in the case of the sensor, is the plate where the electrodes reside. Impaction is defined by the Stokes number:

$$Stk = \frac{\rho_p d_p^2 V C_c}{9 \mu_g D_j}$$

*Where:*

*$\rho_p$: particle density [kg/m³]*
*$d_p$: particle equivalent diameter [m]*
*$C_c$: Cunningham slip correction factor [-]*
*$\mu_g$: dynamic viscosity of the gas [Ns/m²]*
*V: exhaust gas velocity [m/s]*
*$D_j$: characteristic length which is the half-width of the gas stream that collides on the plate [m]*

The impaction efficiency $E_I$ gives the fraction of entering particles deposited:

$$E_I = \frac{\pi}{2} \cdot Stk$$

Thermophoresis

When a temperature gradient is established in a gas, a force is applied on an aerosol particle in the direction of decreasing temperature. The thermophoretic velocity is defined from the equation:

$$V_{th} = -K_{th} \frac{v_g}{T} \nabla T$$

*Where:*

*$v_g$: kinematic viscosity of the gas [m²/s]*
*T: temperature of the particle [K]*
*$K_{th}$: thermophoretic coefficient*

The thermophoretic coefficient, as defined by (9), is given by:

$$K_{th} = \frac{2 C_s C_c}{1 + 3 C_m \left(2\lambda / d_p\right)} \cdot \frac{k_g / k_p + C_t \left(2\lambda / d_p\right)}{1 + 2 k_g / k_p + 2 C_t \left(2\lambda / d_p\right)}$$

*Where:*

*$k_g/k_p$: the ratio of gas-to-particle thermal conductivity [-]*
*$d_p$: particle equivalent diameter [m]*
*$\lambda$: mean free path of gas [m]*
*$C_s$: thermal creep coefficient, equal to 1.17 [-]*
*$C_t$: temperature jump coefficient, equal to 2.18 [-]*
*$C_m$: velocity jump coefficient, equal to 1.14 [-]*
*$C_c$: Cunningham slip correction factor [-]*

The thermophoretic force which is applied to the particle is in turn calculated by the following equation (10):

$$F_{th} = V_{th} \frac{m_p}{\tau_v}$$

*Where:*

*$V_{th}$: thermophoretic velocity [m/s]*
*$m_p$: particle mass [kg]*
*$\tau_v$: particle relaxation time [s],*

The particle relaxation time is expressed as:

$$\tau_v = \frac{\rho_p d_p^2 C_c}{18 \mu_g}$$

*Where:*

*$\rho_p$: particle density [kg/m³]*
*$d_p$: particle equivalent diameter [m]*
*$C_c$: Cunningham slip correction factor [-]*
*$\mu_g$: dynamic viscosity of the gas [Ns/m²]*

Electrophoresis

Large fraction of particles, approximately 60-80% are electrically charged, but with nearly equal positive and negative charges (11). Near the electrodes of the sensor, an electric field exists which attracts or repels any charged particle. The intensity of this field is significant enough and needs to be taken into account. When a charged particle is placed in an electric field, then an electrostatic force is applied:

$F_E = neE$ Where: *ne: the charge of the particle expressed as a number (n) of elementary units of electron charge (e)*
*E: field intensity [N/C]*

Brownian Diffusion

A particle concentration gradient causes a continuous diffusion of aerosol particles to the surface (7). This gradient exists in proximity of the electrodes; on the surface, the aerosol concentration is always zero, because the particles adhere where they collide (7). The first Fick's law is defined by (10):

$J_p = -D \cdot \nabla n$ Where: *$J_p$: particle deposition flux [(number of particles) / (m²s)]*
*$\nabla$ n: concentration gradient [(number of particles/m]*
*D: diffusion coefficient of particles [m²/s]*

The diffusion coefficient is determined from (10):

$$D = \frac{k_B T C_c}{3\pi\mu_g d_p}$$ Where: *$k_B$: Boltzmann's constant [J/K]*
*$d_p$: particle equivalent diameter [m]*
*$C_c$: Cunningham slip correction factor [-]*
*$\mu_g$: dynamic viscosity of the gas [Ns/m²]*

## 3. EXPERIMENTAL SETUP

To assess the effect of the deposition mechanisms to the soot sensor response time, a group of measurements has been designed and conducted in order to investigate the sensor behavior in a range of conditions of exhaust gas soot concentration, temperature and velocity. Each measurement is a selected steady state point that corresponds to a specific combination of the aforementioned parameters.

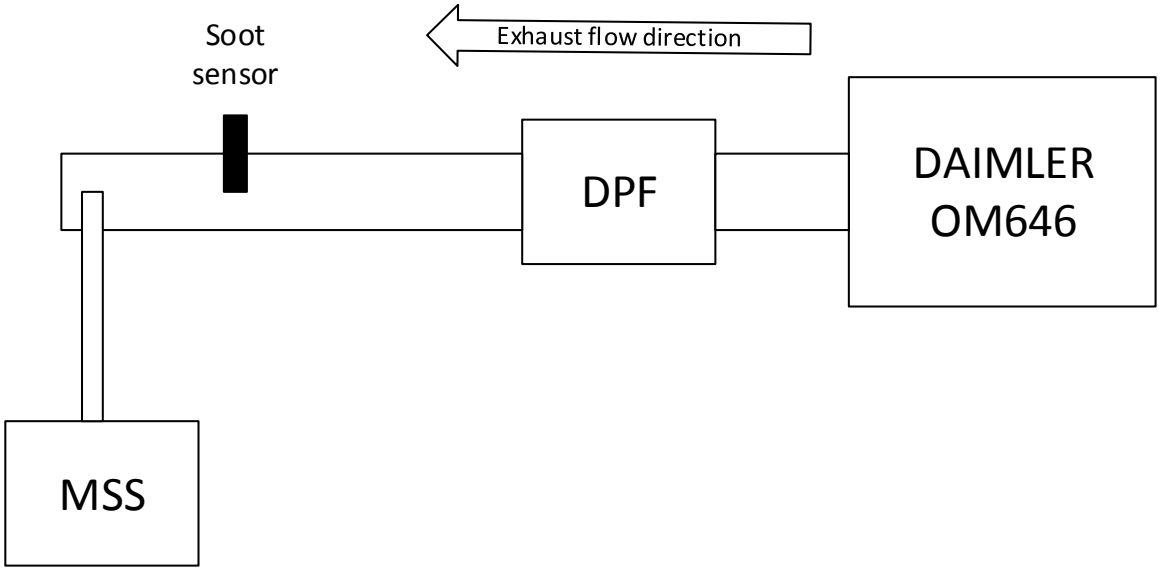

Figure 3 - Simplified schema of the measurement setup

A Micro Soot Sensor (MSS) is used in order to track and record the instantaneous soot concentration value in the exhaust pipe. A DPF is used downstream the engine, to set the soot concentration in desired range. Typically the soot concentration range is between 2 and 8 mg/m³. All exhaust flow parameters, such as temperature and mass flow are also recorded; these data are used to feed the deposition models. The engine parameters are shown in the table below:

Table 1: Engine's parameters

| *Feature* | *Value* |
|---|---|
| Engine | Daimler 2.2 OM646 |
| Fuel | Diesel |
| Displacement [cc] | 2148 |
| Fuel injection system | Common Rail, DI |
| Max Power [kW/rpm] | 110/4200 |
| Max Torque [Nm/rpm] | 330/2100 |
| Cylinders | 4 |
| Emission standards | Euro 4 |

## 4. MODEL PREPARATION IN ANSA

The flow mentioned above was simulated using ANSYS FLUENT as a CFD solver and ANSA/μETA as pre/post-processor. The reasons why ANSA was selected are the following:

- High quality tetrahedral mesh is required especially at the complex tip geometry
- The powerful "*LAYERS*" tool facilitates the quick and detailed boundary layer meshing
- Easy mesh extrusion down/upstream the sensor to account for variations in exhaust pipe characteristics (curves, length, and diameter)
- Splitting the geometry in parts and meshing the volume of each part independently (in conjunction with the non-conformal interface tool in FLUENT) enables modification of the angle of attack for both the tip and the element in a rapid and efficient way.

Model geometry and mesh metrics

The target of the simulations was to investigate how the sensor tip modifies the velocity and turbulence field around the element. Thus the control volume boundaries were chosen to be the sensor element and tip and a part of the exhaust tube upstream and downstream the sensor. The full geometry is illustrated in Figure 4. In order to enable altering the angle of attack of the sensor tip and element, the control volume has been separated into 3 different parts which are meshed independently. The length of the control volume is 87 mm and the pipe diameter is 55 mm.

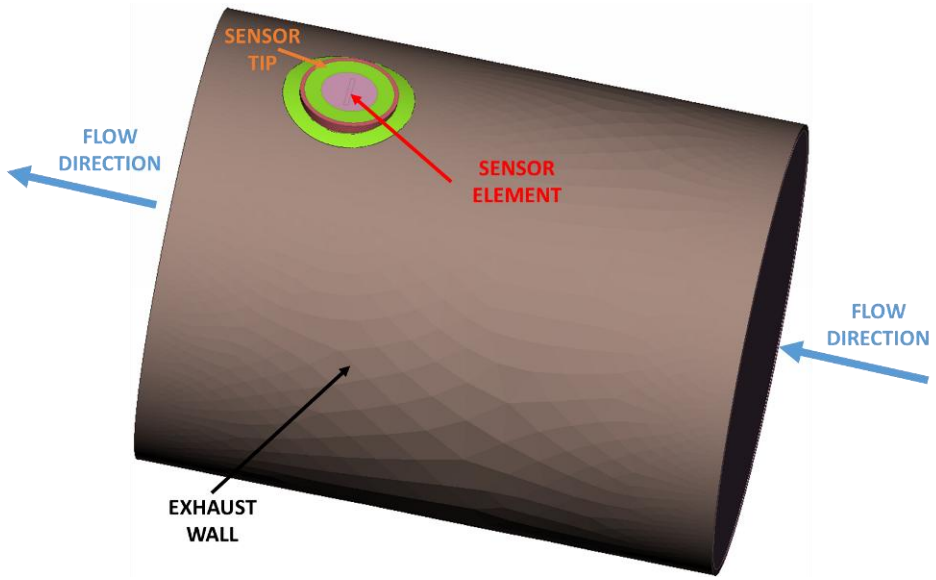


Figure 4 – Full model geometry

In order to avoid convergence issues during the solving phase, the boundaries of the three volumes have been appointed at "low-risk" areas. The three volumes are illustrated in Figure 5, while the number and type of cells for each part are listed in Table 2. The first volume ("Exhaust") contains almost the entire volume within the pipe apart from the area that

surrounds the tip (2 mm radius from the tip external surface). The second volume ("sensor tip") includes the area within the exhaust that covers the tip, the tip itself and the internal area of the tip apart from a cylinder of 3.4 mm radius and 10 mm length which is appointed to the "sensor element" volume.

Table 2 – Number of volume cells per part and cell type

| *Part* | *Exhaust* | *Sensor tip* | *Sensor element* | *Model* |
|---|---|---|---|---|
| *"Tetras"* | 144,460 | 267,098 | 32,518 | 553,978 |
| *"Pentas" (layers)* | 81,080 | 191,588 | 20,260 | 292,928 |
| *Solid "tetras"* | - | 109,902 | 6,400 | 6,400 |
| *Total cells* | 225,540 | 568,588 | 59,178 | 853,306 |

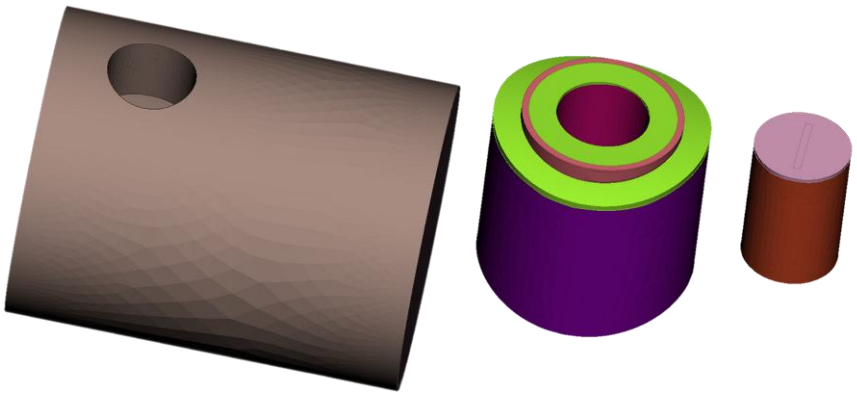

Figure 5 – The volume parts from left to right: "Exhaust", "Sensor tip", "Sensor element"

Geometry meshing – Layers generation

Like most CFD models, special mesh treatment is needed at the wall boundaries in order to maintain $y^+$ at specific levels (either $y^+<1$ or $y^+\sim50$) and thus utilise the built-in wall functions in FLUENT for simulating the flow field at the boundary layer. Since the model is divided into three independent volumes, the boundary layer mesh was formed in each volume with different parameters taking into account the average flow velocity in each one. In order to evaluate the flow velocity in the tip for the $y^+$ calculation, prior to the simulation, it was assumed that the gas flow rate in the tip is relative to the exhaust flow rate. The relation between the two velocities is the ratio of the inlets (tip/exhaust) cross-sections. The formation of layers for the "Exhaust" volume is a relatively easy task with the "*LAYERS*" tool in ANSA. The first layer height is set to 0.1 mm and the number of layers is set to 5 (absolute). Layers grow from the exhaust pipe wall and the interface between the "Exhaust" and "Sensor tip" volume. The quality criteria used for the mesh in the layers and the whole model are the following: *skewness (0.92), min/max angle pentas (30/0.92), jacobian (0.4), squish (0.95) and negative* volume.

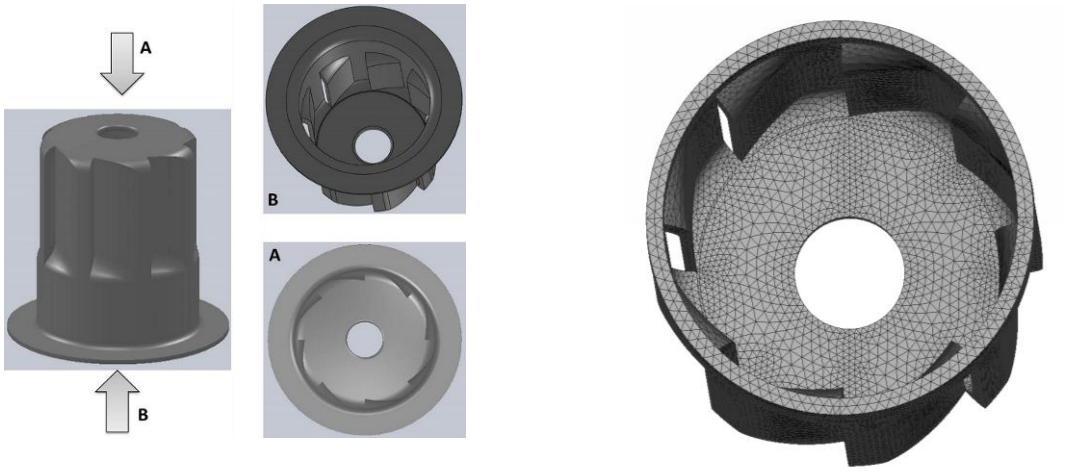


Figure 6 – The sensor tip geometry (left) and mesh in ANSA (right)

The layer generation in the “Sensor tip” part is the most tedious as the tip geometry is elaborate comprising of a cylinder with 9 openings in general. There are 8 peripheral openings with tangential direction. These openings provoke swirl formation within the tip. There is also one additional circular opening at the bottom of the tip (Figure 6). Attempting to generate the layers without customization leads to errors due to the complexity of the geometry at the peripheral inlets. These areas are highlighted in Figure 7. The issue is resolved by growing layers also from both sides of the 8 inlets regarding them as “*ZERO-THICKNESS WALLS*” in the “*GROW FROM*” command included in the “*LAYERS*” tool in ANSA. The faces that are marked as *ZERO-THICKNESS* grow layers from both face sides.

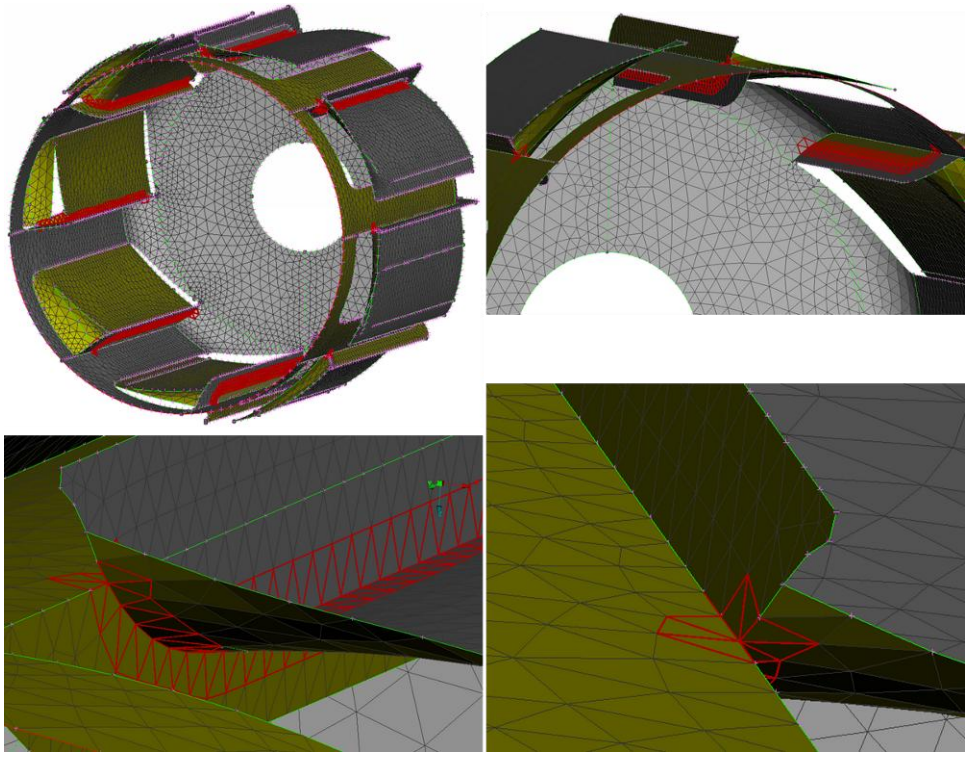

Figure 7 – Problematic areas at the sensor tip inlets marked with red by the *LAYERS* tool

As far as the circular orifice at the bottom of the tip is concerned, the *ZERO-THICKNESS* option is also chosen here in order even though an error does not occur otherwise as in the case of the tangential inlets. However, as shown in Figure 8, if this face is not considered as a *ZERO-THICKNESS WALL*, a void is formed that could lead to mesh errors during the volume meshing of the part. The void cross-section is marked in the same figure with a red triangle. In total, 4 layers of *penta* cells are formed, with the *first layer height* being 0.1 mm (aspect) and all internal faces (openings) are marked with the *ZERO-THICKNESS* option.

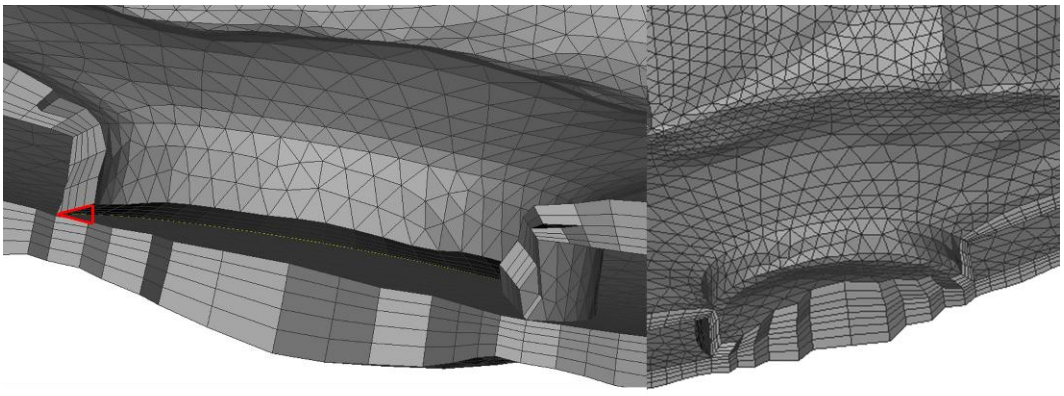

Figure 8 – Layers generation without (left) and with (right) the ZERO-THICKNESS option

The layer generation at the sensor element part is not as complicated as is the case of the sensor tip. Five Layers grow from all the plate's faces and also from the exhaust pipe wall that is included in the part. The *first layer height* is set to 0.2 mm (aspect). After forming the layers, the internal volume meshing was performed with the *MESH>Volumes>Mesh Vol.>Tetra Rapid* option in ANSA. The final result of the model preparation is visible in Figure 10.

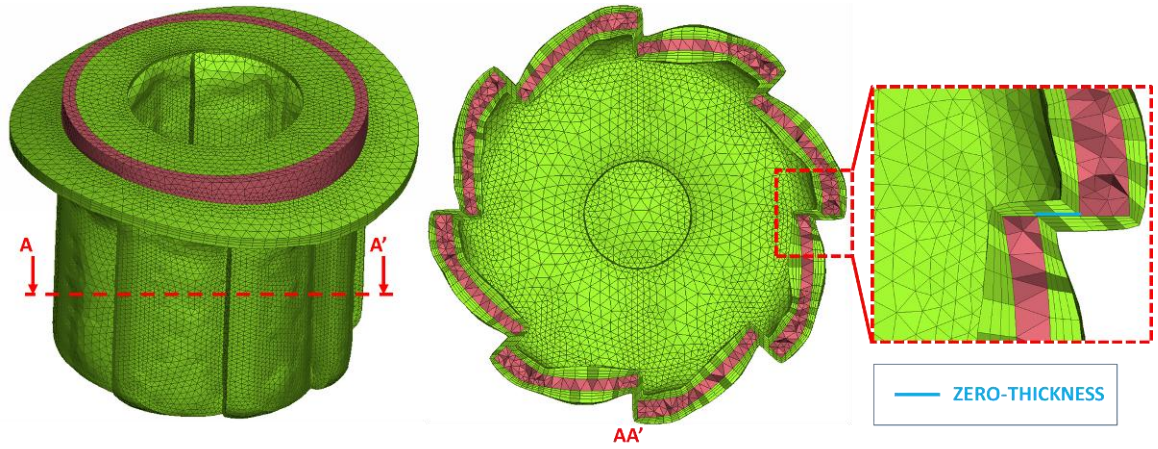


Figure 9 – Layers generation at the sensor tip

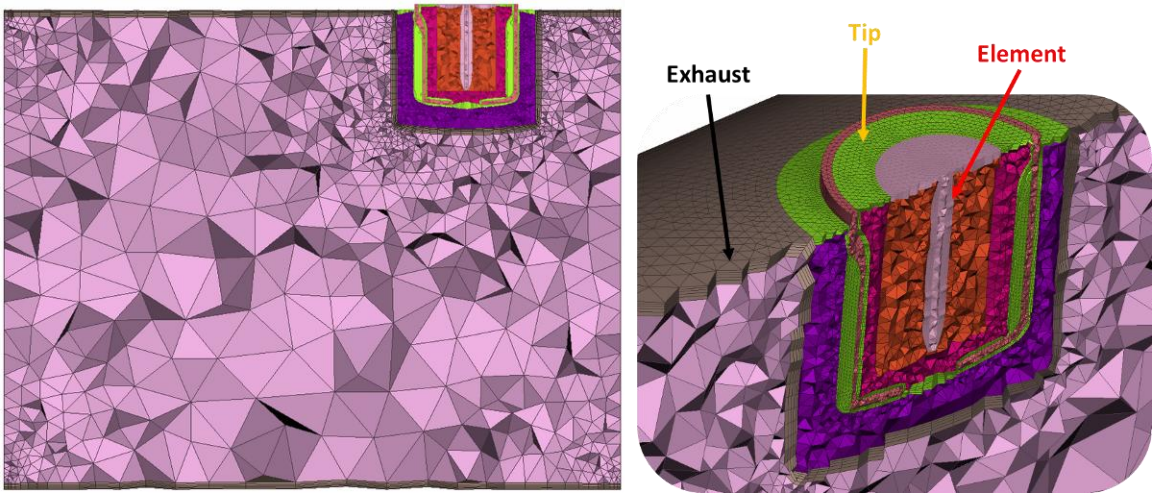


Figure 10 – Model mesh view at the symmetry plane (left) and detailed mesh view at the sensor area (right)

## 5. RESULTS

The 3D model was simulated using FLUENT 14.0. The "*Realizable k-ε*" model is the selected turbulence model. The *"Near-Wall Treatment*" option is the "*Enhanced Wall Treatment"* which is the suitable option for a mesh with $y^+<1$. Since upstream the sensor, the exhaust gas flow is fully developed, a parabolic inlet velocity profile is necessary for better accuracy. The velocity profile was created outside FLUENT in a separate spreadsheet. A constant velocity profile is exported from FLUENT, it is manipulated externally and the updated velocity profile is imported into FLUENT and appointed as inlet condition.
The mesh shown in Figure 10, is the final mesh used for the coupled simulations. In order to reduce calculation times, part of the mesh downstream the sensor has been removed. In order to accomplish this without affecting the flow field an initial mesh with an extended downstream mesh (extension length is 35 mm) has been created and solved in FLUENT. During this calculation, the solution data at the cross-section located 11 mm downstream the sensor is recorded and are used as input at the *outlet* boundary of the reduced mesh. The

results of both meshes have been compared to validate the results of the reduced mesh. A 21% reduction in calculation time is achieved.
The model has been solved for four different inlet velocities representing idle, partial loads and full load engine operation. The *Solution* parameters used in FLUENT are: *Scheme: Coupled (Courant number = 10), Spatial Discretization parameters: Green-Gaus Node Based (Gradient), PRESTO! (Pressure), QUICK (Momentum), Second Order Upwind (Turb. Kin. Energy, Turb. Diss. Rate & Energy)*.

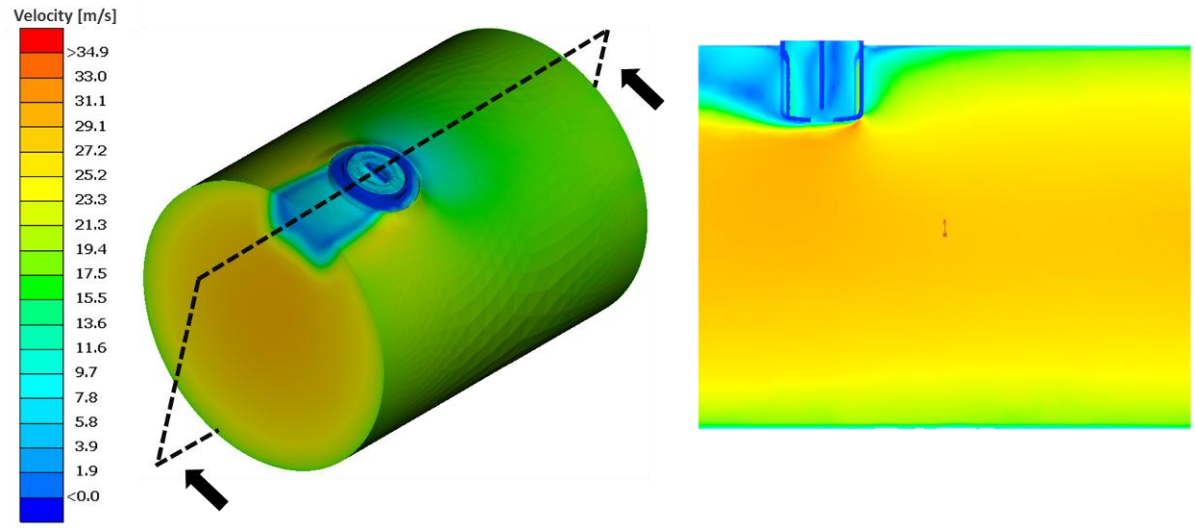


Figure 11 – Full mesh velocity contour (left) and at the longitudinal symmetry plane (right – using the "*Cut Planes*" tool in μETA)

Through the 3D simulations at FLUENT, the flow field around the sensor element is calculated and the solution data are the input of the 1D soot deposition model. An overview of the control volume flow field is represented in Figure 11. The solution data acquired through the FLUENT model runs, provide a visualisation of the flow field within the sensor and also velocity and turbulence data at the sensor element.

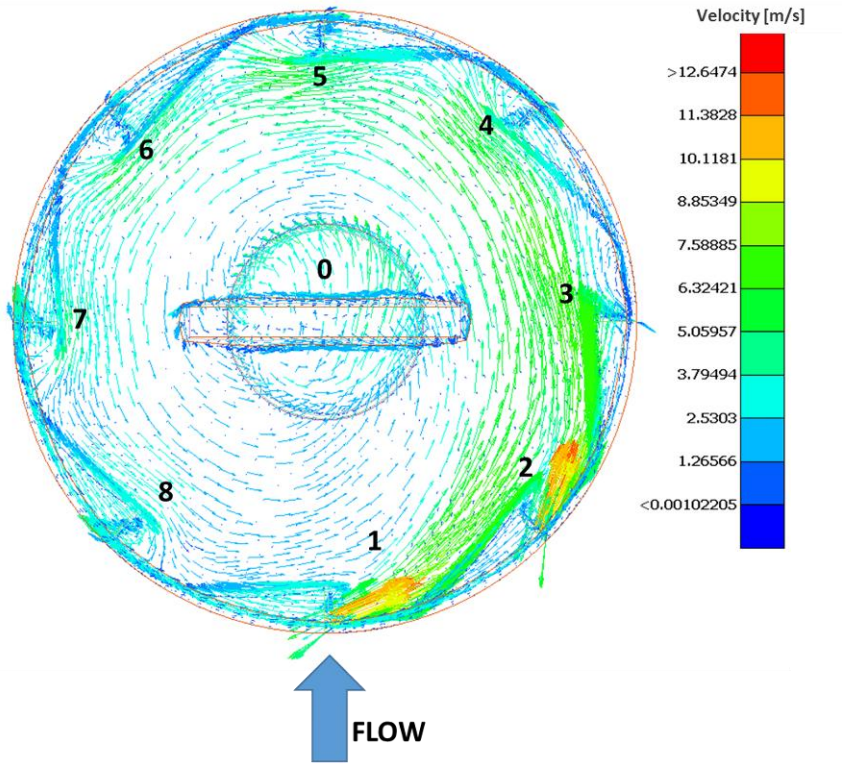


Figure 12 – Velocity vectors in the sensor tip

As illustrated in Figure 12, the sensor tip forms a swirling flow at the interior that tangentially flows around the element. This way, the axial velocity at the front of the element is minimised, as is the dynamic pressure and bending force on the plate. In the same figure it is also visible that inlets 1,2 and 3 allow gas to flow in the sensor tip. “Inlets 4-8 act as outlets, along with the circular outlet orifice at the edge of the tip. These findings are also validated through the *Flux Report* tool in FLUENT. This flow pattern would not have been identified without the 3D model and moreover, the exact gas velocity and turbulence characteristics at the element could not be efficiently assumed. The velocity and turbulence intensity contours at the front area of the sensor element (the plate) and the velocity vectors are shown in Figure 13.

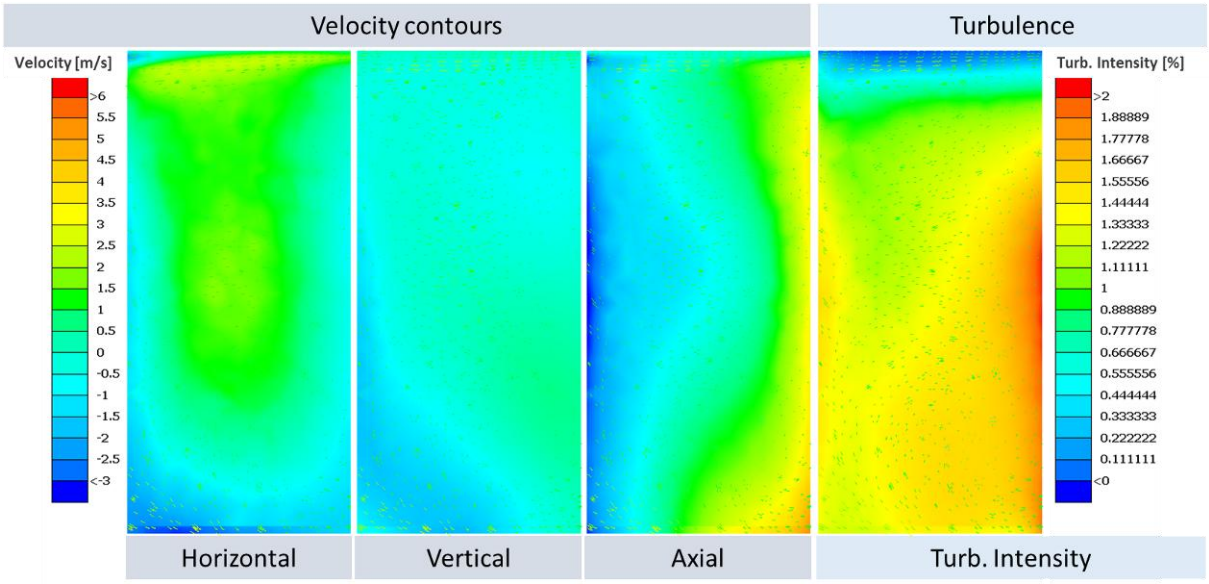


Figure 13 – Velocity and turb. Intensity contours at the sensor element front face (Simultaneous contour and vector plot 1 mm upstream the element)

The examined gas exhaust velocity scenarios range from 6 to 24 m/s. Inside the sensor tip, the exhaust velocity drops to the ~18% of its nominal value, which is the velocity outside the tip. This assumption of exhaust velocity inside the tip, significantly affects all deposition mechanisms and thus the sensor response time. Besides, the mass flow of the exhaust gas drops almost three orders of magnitude inside the tip.

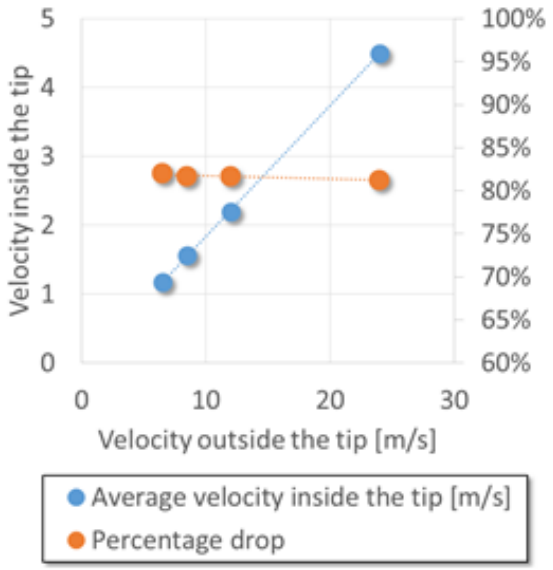


Figure 14 – Velocity and mass flow drop inside the sensor tip

Turbulent intensity modelled by the 3D model is in all cases low enough to assume that the turbulent impaction is negligible and does not affect the sensor response time. The solution data from the 3D model are introduced into the soot deposition model which has been developed in C# and FORTRAN. The deposition model seems to correctly predict the soot value signal in most cases. In Figure 15, the behavior of a prototype soot sensor has been predicted for a steady state point of soot concentration 2 mg/m³ and exhaust velocity 12 m/s.

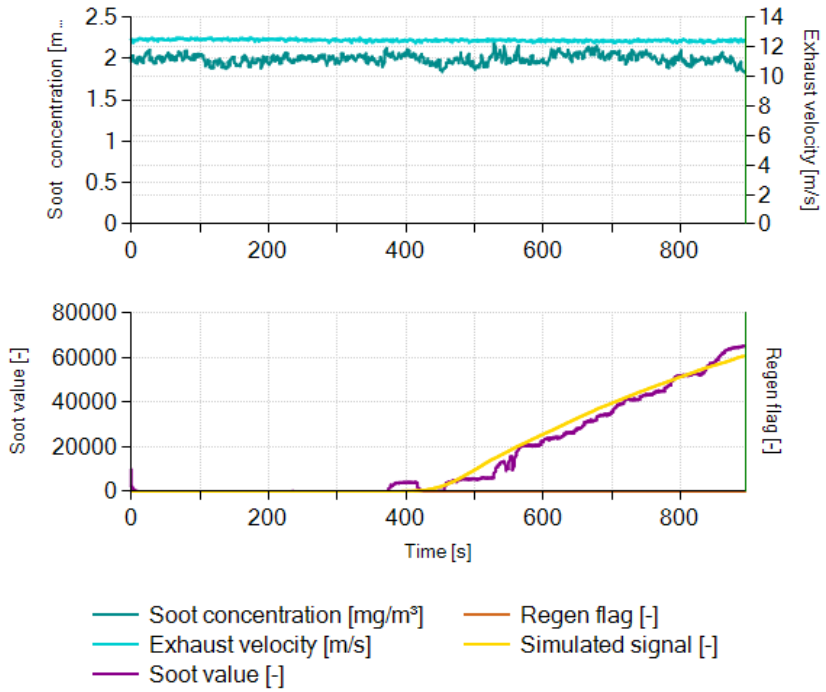


Figure 15 Simulated vs Real sensor signal (Soot value)

For some cases (Figure 16) where the soot concentration is quite unstable, the simulated signal (yellow line) may overestimate or underestimate the accumulation rate of the soot.

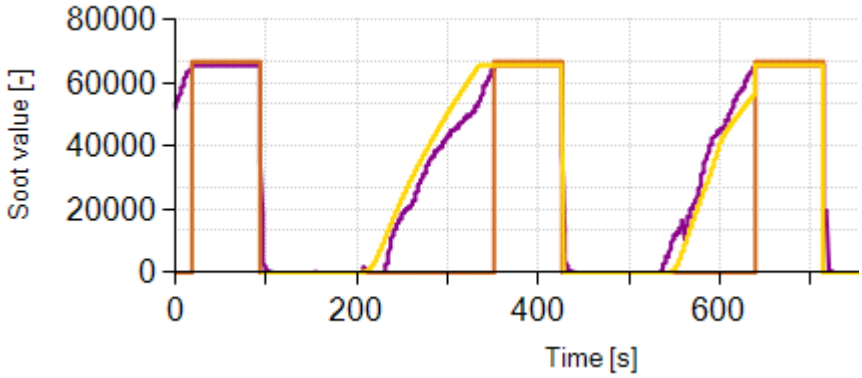


Figure 16 Overestimate and underestimate of the Soot Sensor signal (yellow is the simulated and purple is the real sensor signal).

## 6. CONCLUSIONS

The modelling of the behaviour of resistive soot sensors can greatly assist in the direction of more efficient DPF control in passenger vehicles. The variation in exhaust pipes and soot sensor tips is a pain towards the successful modelling. Towards this direction a 3D CFD model has been developed aiming at providing accurate data regarding the flow field inside the soot sensor. By examining a specific sensor tip flow via CFD and feeding the CFD output data to a physical deposition model of the soot particles inside the sensor, the sensor signal output can be estimated for steady state points. The contribution of ANSA during the 3D

model preparation is twofold: a) accurate and rapid meshing of a complex geometry such as the sensor tip and, b) splitting the geometry into separate parts that are meshed and modified independently to test variations in the flow characteristics (angle of attack, pipe diameter etc). The 3D model is simulated in FLUENT 14 and the post-process of the solution data is performed using the μETA-postProcessor.

## REFERENCES


(1) ANSA version 15.1.x User's Guide, BETA CAE Systems S.A., June 2014

(2) μETA version 15.1.x. User's Guide, BETA CAE Systems S.A., June 2014

(3) Berger J, Strohmaier R et al., Sensor For Detecting Particles, US Patent No. 7,543,477 B2, June 8, 2009

(4) Acchammer, R., Ante J. et al., Soot Sensor, US Parent No. 2011/0156727 A1, June 30, 2011

(5) Masoudi M., Sappok A., Soot (PM) Sensors, DieselNet Technology Guide, Ecopoint Inc. Revision 2014.07, available at: www.dieselnet.com/tech/dpf_soot_sensors.php

(6) Ochs, T., Schittenhelm, H., Genssle, A. and Kamp, B., Particulate Matter Sensor for On Board Diagnostics (OBD) of Diesel Particulate Filters (DPF), SAE Technical Paper 2010-01-0307, 2010

(7) Hinds, William, Aerosol Technology, Second Edition, John Wiley & Sons, 1999

(8) Friedlander, Sheldon, Smoke, Dust, and Haze Fundamentals of Aerosol Dynamics, Second Edition, Oxford University Press, 2000

(9) Talbot, L., Cheng, R. et al., Thermophoresis of Particles in a Heated Boundary Layer, J. Fluid Mech. 101:737-758, 1980

(10) Crowe, Clayton, Multiphase Flow Handbook, Taylor & Francis, 2006

(11) Maricq MM., On the electrical charge of motor vehicle exhaust particles, Journal of Aerosol Science 37 (2006) 858-874, 2005